MOLECULAR AND CELLULAR BIOLOGY, Nov. 2008, p. 6731–6745 Vol. 28, No. 22
0270-7306/08/$08.00+0 doi:10.1128/MCB.02103-07

A Novel *H19* Antisense RNA Overexpressed in Breast Cancer Contributes to Paternal *IGF2* Expression▽†

Nathalie Berteaux,[1,3] Nathalie Aptel,[2] Guy Cathala,[2] Céline Genton,[2] Jean Coll,[3] Anthony Daccache,[3] Nathalie Spruyt,[3] Hubert Hondermarck,[1] Thierry Dugimont,[1] Jean-Jacques Curgy,[1] Thierry Forné,[2] and Eric Adriaenssens[1]*

INSERM U908, IFR 147 and Université Lille1, 59655 Villeneuve d'Ascq, France[1]; Institut de Génétique Moléculaire, CNRS UMR 5535, Université Montpellier II, IFR 122, Montpellier, France[2]; and CNRS UMR 8161, IBL, Universités de Lille I et Lille II, Institut Pasteur, Lille, France[3]

Received 26 November 2007/Returned for modification 14 January 2008/Accepted 29 July 2008

The *H19*/*IGFf2* locus belongs to a large imprinted domain located on human chromosome 11p15.5 (homologue to mouse distal chromosome 7). The *H19* gene is expressed from the maternal allele, while *IGF2* is paternally expressed. Natural antisense transcripts and intergenic transcription have been involved in many aspects of eukaryotic gene expression, including genomic imprinting and RNA interference. However, apart from the identification of some *IGF2* antisense transcripts, few data are available on that topic at the *H19*/*IGF2* locus. We identify here a novel transcriptional activity at both the human and the mouse *H19*/*IGF2* imprinted loci. This activity occurs antisense to the *H19* gene and has the potential to produce a single 120-kb transcript that we called the *91H* RNA. This nuclear and short-lived RNA is not imprinted in mouse but is expressed predominantly from the maternal allele in both mice and humans within the *H19* gene region. Moreover, the transcript is stabilized in breast cancer cells and overexpressed in human breast tumors. Finally, knockdown experiments showed that, in humans, *91H*, rather than affecting *H19* expression, regulates *IGF2* expression in *trans*.

H19 is located within a cluster of imprinted genes on the human chromosome 11 in p15.5 (homologue to the murine distal chromosome 7). The regulation of *H19* and its closely linked and reciprocally imprinted neighbor, *IGF2*, has been studied intensively both because of its role in human diseases and as a model for understanding imprinting control mechanisms. Thereby, *H19* is transcribed only from the maternal allele, whereas *IGF2* expression is exclusively paternal (8). Over the years, *H19* is considered as a regulatory RNA (5). It has been proposed to function in many different processes, ranging from transcriptional and posttranscriptional regulation (25, 26, 53) to tumor suppression (35, 45) and oncogenesis, more particularly in breast cancer (1, 27, 28).

Genomic imprinting plays a critical role in modulating gene expression during embryogenesis and normal development (36). It consists of an epigenetic modification that results in the silencing of a specific allele, depending on its parental origin. Most of the 80 mammalian imprinted genes identified thus far are organized into clusters (33). It has been suggested that the clustering of genes enables sharing of *cis*-acting elements located several kilobase pairs away (21). Differentially methylated regions associated with the imprinted clusters play a crucial role in the imprinted expression patterns, which are hence called imprinting control regions (ICRs) (22, 38). The *H19*/*IGF2* locus is a well-characterized cluster. Both genes share a common set of enhancers located downstream from the *H19* gene. The ICR, located 2 kb upstream of the *H19* promoter, controls the monoallelic expression of the *H19* and *IGF2* genes by insulating communication between the 3′ enhancers and the *IGF2* promoter. The chromatin insulator property of the *H19*/*IGF2* ICR is regulated by a chromatin insulator protein, CTCF (for CCTC-binding factor), which binds only the nonmethylated maternal allele. On the paternal allele, the ICR methylation does not allow CTCF binding and leads to *IGF2* expression (for a review, see reference 24). The *IGF2* gene itself also contains differentially methylated regions (DMRs), with DMR1 being a methylation-sensitive silencer and DMR2 being a methylation-sensitive activator (7, 30). Elsewhere, the role of CTCF in chromatin loops is now well demonstrated. Indeed, CTCF binding in the maternal ICR is able to regulate its interaction with matrix attachment region 3 (MAR3) and DMR1 at *IGF2*, thus forming a tight loop around the maternal *IGF2* locus which may contribute to its silencing. These interactions may contribute to restrict the physical access of distal enhancers to *IGF2* promoter (19, 30, 50). Additional mechanisms exist for an imprint mark, such as chromatin composition, organization, and histone acetylation or methylation state (12, 14), even if DNA methylation is by far the best candidate (4).

A more recently identified characteristic of imprinted genes is their association, in some cases, with noncoding antisense transcripts (ncRNAs), which have been suggested to constitute a new epigenetic regulatory system. Indeed, for the maternally expressed *Igf2r* and *UBE3A* genes, overlapping antisense transcripts have been found and are oppositely imprinted with respect to the protein coding gene. It has been proposed that antisense transcripts serve to regulate overlapping genes by promoter or transcript occlusion or by competing with these

* Corresponding author. Mailing address: INSERM U908, Université des Sciences et Technologies de Lille, Bâtiment SN3, 59655 Villeneuve d'Ascq Cedex, France. Phone: 33 320 43 40 14. Fax: 33 320 43 40 38. E-mail: eric.adriaenssens@univ-lille1.fr.

† Supplemental material for this article may be found at http://mcb.asm.org/.

▽ Published ahead of print on 15 September 2008.

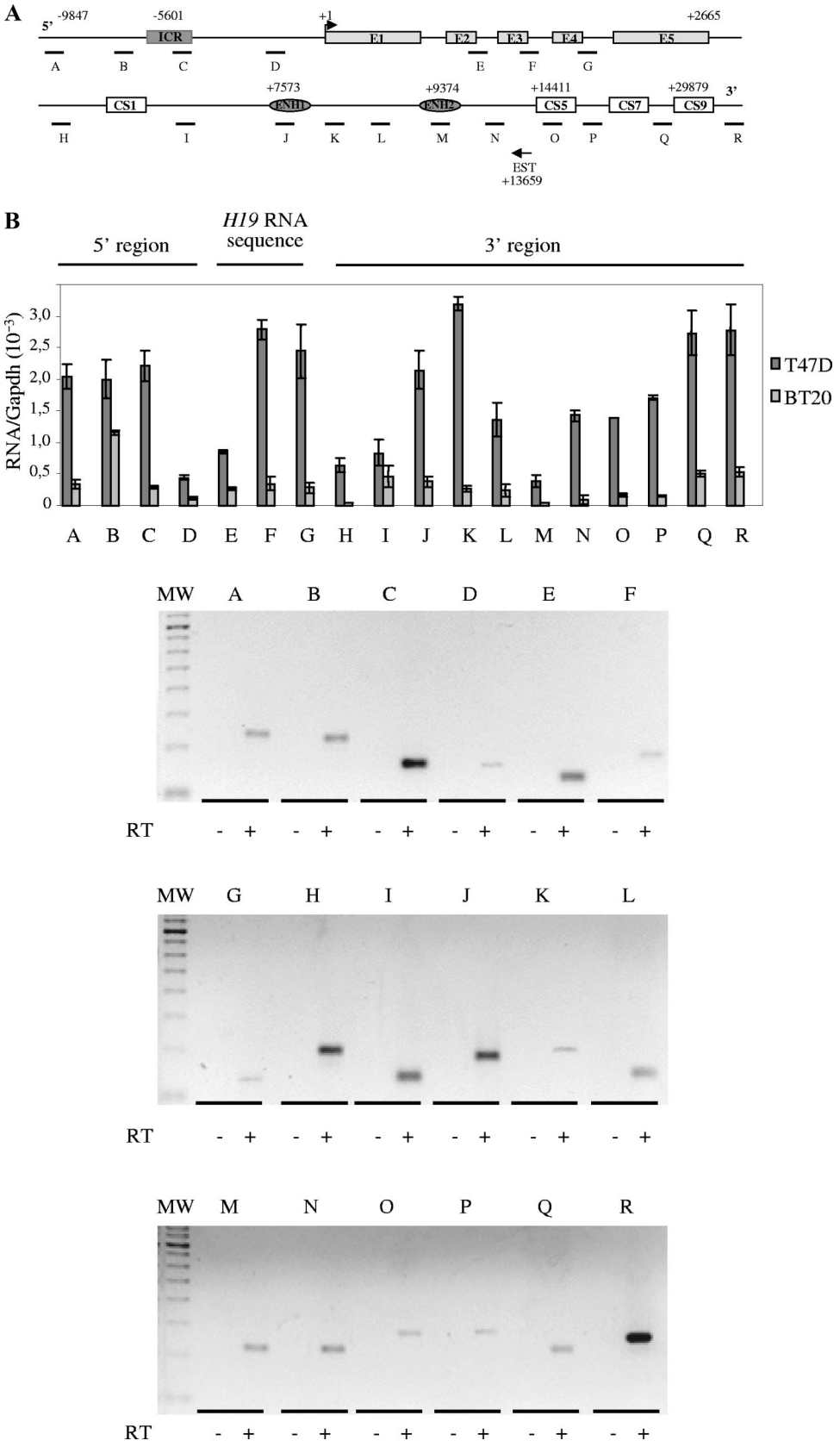
A
5' -9847
-5601
+1
+2665
ICR
E1
E2
E3
E4
E5
A B C D E F G
+7573
+9374
+14411
+29879
3'
CS1
ENH1
ENH2
CS5
CS7
CS9
H I J K L M N O P Q R
EST
+13659
B
5' region
H19 RNA sequence
3' region
RNA/Gapdh (10-3)
3,0
2,5
2,0
1,5
1,0
0,5
0
T47D
BT20
A B C D E F G H I J K L M N O P Q R
MW A B C D E F
RT - + - + - + - + - + - +
MW G H I J K L
RT - + - + - + - + - + - +
MW M N O P Q R
RT - + - + - + - + - + - +

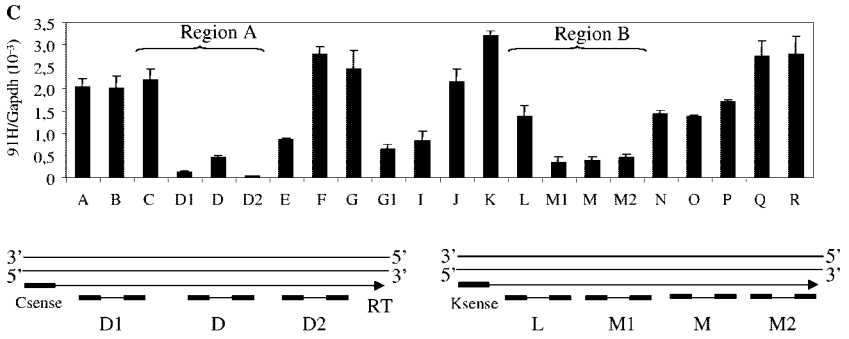

PCRprimers	Ct
M	27.96
G	28.22
Mb	28.88

PCRprimers	Ct
L	33.84
M1	32.70
M	33.65
M2	32.34

FIG. 1. Detection of an intergenic transcriptional activity at the *H19* locus in cancer cell lines. (A) Map of the *H19* gene locus. The relative positions of the real-time PCR amplification fragments (A to R) are depicted in the map. CS represents conserved regions between mice and humans that possess enhancer activities (17). Black arrow represents a known EST that was identified after alignment of the human chromosome 11 sequence with EST databases. EST, BX 377296 cDNA source placenta. (B) Quantification of RNA levels were determined by real-time RT-PCR on total RNA samples in T47D and BT20 cell lines. The results were normalized to *GAPDH* expression levels. Agarose gel shows the amplification products obtained after the real-time PCR on T47D cells. Note that amplifications E to G may also potentially quantify *H19* precursors RNAs. (C) Strand-specific RT in two regions showing a decrease of *91H* transcription (region 1 and region 2). Antisense-specific RT analyses were performed with the primer C sense in region 1 and K sense in region 2. Transcription was detected by PCR using several contiguous primer pairs (D1, D, and D2 for region 1 and L, M1, M, and M2 for region 2). Results, expressed in terms of the cycle threshold (Ct) are indicated in the lower part of panel C. Cycle threshold values that are equivalent for all primer pairs indicate that there is no transcriptional arrest in both tested regions. Primer sequences are available in Table S1 in the supplemental material.

loci for regulatory elements such as transcription factors or enhancers (39, 40, 44, 54). Elsewhere, in the imprinted cluster at the distal end of the mouse chromosome 7 (orthologous to the human chromosome 11), the ICR located in the *KCNQ1* gene contains the promoter of a long paternally expressed antisense transcript called *KCNQ1OT1*. This transcript takes part in gene silencing of the *KCNQ1* domain, and its interruption by the insertion of a polyadenylation sequence caused a loss of methylation spreading in cultured cells (31, 47).

These ncRNAs are not yet clearly classified, but categories with known gene regulatory functions are emerging. It includes intergenic transcripts that regulate local chromatin activity, *cis*-acting long ncRNAs such as *Xist* involved in chromosome inactivation, and the imprinted *Air* and *KCNQ1OT1* ncRNAs involved in domain silencing (15, 32).

In the present study we have identified and characterized a new transcript within the human and mouse *H19/IGF2* locus. This long intergenic RNA that we named *91H* is antisense to *H19*. We assessed the effect of the *91H* knockdown by RNA interference on genomic imprinting and on *H19* and *IGF2* gene expression. The results reported here add further complexity to the locus regulation and are attractive within the context of imprinting maintenance and/or cancer development.

MATERIALS AND METHODS

Cell culture and breast tissues. The estrogen-sensitive MCF7 and T47D and the estrogen-insensitive BT20 human cancerous mammary epithelial cell lines were obtained from the American Type Culture Collection and maintained routinely in minimal essential medium containing 5% fetal calf serum (FCS). The prostate carcinoma PC3 cell line, provided by N. Prevarskaya, was grown in RPMI medium containing 5% FCS. All cell lines were incubated at 37°C in a humidified atmosphere with 5% CO_2 and 95% air. Normal breast epithelial cells (NBEC) came from primary culture of normal breast tissue resections obtained from modeling surgery. The mouse skeletal muscle cell line C2C12 was grown in 50% Dulbecco modified Eagle medium, 50% Ham's F-12 containing 10% FCS. Myoblastic differentiation was induced by serum starvation. When cells reached 70% confluence, FCS was reduced to 1%, and the differentiated cells were recovered after 72 h. For RNA stability assays, actinomycin D at 5 μg/ml was added to the growth medium for the times indicated in the figure legends. Breast cancer tissues came from biopsies corresponding to intraductal cancers.

RNA extraction. Total RNA was extracted with Tri-Reagent (Euromedex) and treated for 1 h at 25°C with amplification-grade RNase-free DNase I (Invitrogen) or isolated by using a Nucleospin RNAII isolation kit (Macherey-Nagel).

Reverse transcription. Total reverse transcriptions were performed as follows: 1 μg of RNA, 4 μl of buffer containing random hexamers, and 1 μl of reverse transcriptase (RT; Bio-Rad) were incubated for 5 min at 70°C, for 30 min at 37°C, and for 5 min at 85°C in a final volume of 20 μl. For strand-specific reverse transcription, we used the Thermoscript RT-PCR System (Invitrogen). A total of 2 μg of total RNA was incubated 5 min at 65°C with a 1 μM concentration of the primer and a 10 μM concentration of deoxynucleoside triphosphate in a final volume of 12 μl. We then added 4 μl of buffer (5×), 1 μl of dithiothreitol (0.1 M), 1 μl of RNase Out (40 U/μl), and 2 μl of H_2O. The sample was divided into two equal parts. Thermoscript (1 μl) was added in one of them (+RT), and 1 μl of H_2O was added to the other to constitute the negative control (–RT). The reverse transcription was performed 20 min at 60°C to improve specificity. The reaction was stopped by 5 min at 85°C, and cDNA/RNA duplexes were removed by the addition of 1 μl of RNase H for 15 min at 37°C. The primer used for *H19*-specific RT is referred to as "H19-specific RT," and the primer used for *91H* specific RT is referred to as U'sense (Table S1 in the supplemental material).

Real-time RT-PCR. Real-time PCR amplifications were performed by using a QuantiTect Sybr green PCR kit (Qiagen) with 2 μl of cDNA and 500 nM concentrations of the primers. The primers used for the *H19* transcript, *RPLP0* (for human acidic ribosomal phosphoprotein P0), *GAPDH*, *U3snoRNA*, *MRPL23 mRNA*, and *91H* RNA (D and I) are described in Table S1 in the supplemental material. Other primer sequences are available upon request. The subsequent PCR conditions consisted of 40 cycles of 95°C for 15 s, 60°C for 20 s, and 72°C for 30 s. The data were analyzed by using an MX4000 PCR system software

(Stratagene) with the Sybr green option (with dissociation curves). Standard curves were performed on serial dilutions of a PCR product for *H19* and on serial dilutions of genomic human DNA for *RPLP0*. Values were obtained by the calculation methodology recommended by Pfaffl (34): ratio = $(NC - b/a)_{target}/(NC - b/a)_{reference}$, where *a* is the slope of the standard curve and *b* is the ordinate of origin.

5′RACE- and 3′RACE-PCR. Transcription start site and 3′ end of the *91H* transcript were determined by using RACE (rapid amplification of cDNA ends)-PCR experiments. A Smart RACE cDNA amplification kit (Clontech) was used according to the manufacturer's instructions with cDNA from T47D cells. Primers used for PCR and nested PCR were available upon request. PCR products were amplified with Titanium *Taq* DNA polymerase. RACE-PCR products were characterized by cloning and sequencing. For the 5′RACE, since the transcript is 120 kb in length, we performed the reverse transcription with a specific primer and not with the conventional oligo(dT). The genomic sequence upstream of the transcription start site was tested for promoter elements by using the TFsearch (http://molsun1.cbrc.aist.go.jp/research/db/TFSEARCH.html) (16) and AliBaba (http://www.gene-regulation.com/pub/programs.html) (13) programs.

Analysis of *H19* and *Igf2* restriction fragment length polymorphisms. PCRs encompassing AluI and ApaI sites for *H19* and *IGF2*, respectively, were performed on genomic DNA (gDNA), cDNA of nontransfected cells, or cDNA of small interfering RNA (siRNA)-transfected cells. The primers used were HP1 and HP2 for *H19* and Igf2ApaI sense and Igf2ApaI antisense for *IGF2* (see Table S1 in the supplemental material). PCR conditions were carried out in the following manner: 38 cycles of 94°C for 30 s, 60°C for 30 s, and 72°C for 30 s for *IGF2* and 38 cycles of 94°C for 30 s, 59°C for 30 s, and 72°C for 40 s for *H19*. Then, 15 μl of the PCR product was used for digestions with 2 μl of enzyme buffer 10×, 0.5 μg of bovine serum albumin/μl, and 10 U of the appropriate enzyme for 1 h at 37°C. For AluI polymorphism, digestion of the gDNA-derived PCR product yielded 228-, 128-, and 100-bp bands indicating heterozygosity. The cDNA restriction pattern corresponds to a 148-bp fragment in the allele that lacks the AluI site or two bands of 100 and 48 bp for the allele with the recognition site. For *IGF2*, ApaI digestion generates a 292-bp fragment in the allele without the recognition site or 218- and 74-bp fragments in the allele with the site.

Isolation of nuclei. Nuclei were isolated from human T47D cells and from proliferating and confluent murine C2C12 cells in growth medium and after 1 and 3 days in differentiation medium as follows. First, 10^6 cells were washed twice with phosphate-buffered saline (PBS). The cell layer was scraped into 500 μl of PBS and centrifuged 5 min at 1,200 × *g*. The supernatant was cleared, and this wash step was performed twice. The pellet was estimated to a volume (V) and resuspended in 5V of buffer A (TEA, 10 mM; KCl, 10 mM, $MgCl_2$, 2.5 mM; dithiothreitol, 0.5 mM). After centrifugation under previously described conditions, the pellet was resuspended in 2V of buffer A and disrupted by using a Dounce homogenizer. The separation of nuclei from cytoplasmic compartments was done by centrifugation for 5 min at 3,000 × *g*. The supernatant containing cytoplasmic extracts was resuspended in 5V of Tri-Reagent. The pellet containing the nuclear extracts was washed in 5V buffer A and centrifuged as previously. The pellet was finally resuspended in 5V of Tri-Reagent. Both extracts were maintained at 4°C before RNA extractions. The efficiency of the fractionation was assessed by quantifying two cytoplasmic mRNAs (*RPLP0* and *GAPDH*) and a nuclear RNA (*snoRNA U3*). We analyzed the RNA levels of two cytoplasmic control genes. About 80% of these RNA are detected in the cytoplasm. These data demonstrate the efficient separation of cellular compartments and the absence of contamination from one compartment to the other.

gDNA isolation. A total of 10^7 cells were washed twice with PBS. The cell layer was scraped into 500 μl of physiologic water and then centrifuged for 5 min at 1,000 × *g*. The supernatant was resuspended in 3 ml of STE buffer (Tris-HCl, 10 mM [pH 8.0]; NaCl, 100 mM; EDTA, 1 mM [pH 8.0]). Proteinase K was added at 200 μg/ml. The sample was incubated for 10 min at 37°C. Sodium dodecyl sulfate at a final concentration of 1% was added, and the sample was incubated again for 20 min. gDNA was extracted by addition of an equal volume of saturated phenol and centrifugation for 10 min at 10,000 × *g*. The aqueous phase was collected, and 0.2 M sodium acetate at and 2 volumes of ethanol were added. DNA was rolled up with a Pasteur pipette by mixing progressively the two phases. DNA was finally resuspended in 300 μl of H_2O and stoked at 4°C.

RNA interference. RNA interference was carried out by using synthetic siRNA duplexes, as described by Elbashir et al. (10). Two synthetic siRNA duplexes (si*91H* 1 and si*91H* 2) corresponding to the *91H* RNA sequences 5′-GGCGUC AUUCUGAUGGGACTT-3′ and 5′-UUCAGGAGCUUAAGAUGCUTT-3′, respectively were used to inhibit *91H* RNA expression. A synthetic siRNA duplex (siGFP) corresponding to the green fluorescent protein mRNA sequence (5′-G CUGACCCUGAAGUUCAUCTT-3′) and a sequence corresponding to an intergenic region located at the *H19/IGF2* locus (+108603 bp of the *H19* transcription start site; 5′-CGUGGGUGGAUGCAUGGAUTT-3′) were used as a negative control. The siRNA duplexes were purchased from Eurogentec. Cells were grown on coverslips in six-well plates and transfected with 400 pmol of siRNAs using Jetsi (Eurogentec), as recommended by the manufacturer. To monitor the transfection efficacy, a tagged-siRNA duplex was transfected in parallel, and the transfection rate was evaluated by fluorescence-activated cell sorting and corresponds to 80 to 90% of transfected cells. After transfection, cells were lysed for total RNA isolation.

RESULTS

Intergenic transcriptional activity at the human *H19* locus. Natural antisense transcripts already identified often overlap the 5′ and 3′ intergenic regions of coding sequences. A quick database search allowed us to identify an expressed sequence tag (EST) that corresponds to intergenic sequences that mapped at the human *H19* locus and possessed an antisense orientation (Fig. 1A) (EST, BX 377296, 976 bp, cDNA source placenta). We thus decided to analyze intergenic transcriptional activity at the human *H19* locus. Using a quantitative RT-PCR analysis, we scanned the *H19* locus from sequences upstream of the ICR to sequences downstream of the endodermic enhancers (Fig. 1A). A transcriptional activity was detected throughout the entire region in both the estrogen-sensitive T47D and the estrogen-insensitive BT20 breast cancer cell lines. The produced transcripts have various expression levels according to the cell line (compared T47D and BT20, Fig. 1B). The variations observed throughout the locus in a given cell line were most likely due to differences in the local reverse transcription efficiency. To verify that there were no transcription breaks, we performed near these regions additional specific reverse transcriptions followed by PCR detection. The results obtained indicated that there is no interruption of the transcription and that the variations were due to RT skews (Fig. 1C).

Therefore, in both cell lines, this transcriptional activity overlaps the *H19* RNA sequence and spreads through the 5′ and 3′ intergenic regions, including the ICR and the enhancer regions.

Transcriptional orientation of the intergenic transcriptional activity. We analyzed the transcriptional orientation at four positions flanking the *H19* gene, as well as within the *H19* gene. The principle of the experiments that we performed is described in Fig. 2A (see also Fig. S1A in the supplemental material). Briefly, primer AS allows the detection of transcripts in an antisense orientation to *H19*, while primer S is sense specific. These strand-specific primers were used for reverse transcription on total RNA samples from T47D cells. Real-time PCR amplifications were then performed on each side of the RT primers. At all positions analyzed around (see Fig. S2A in the supplemental material) or within (Fig. 2B and see Fig. S1B in the supplemental material) the *H19* gene, only antisense-specific RT primers (AS primer) gave PCR amplifications. We conclude that, in humans, the detected transcripts are antisense to the *H19* gene. This result is consistent with the data available from the EST described above. It should be noted that, within the *H19* gene, no precursor of *H19* (S primer) could be detected in the same experimental conditions where the antisense transcription is found (Fig. 2B).

Finally, an in situ hybridization signal can be detected with

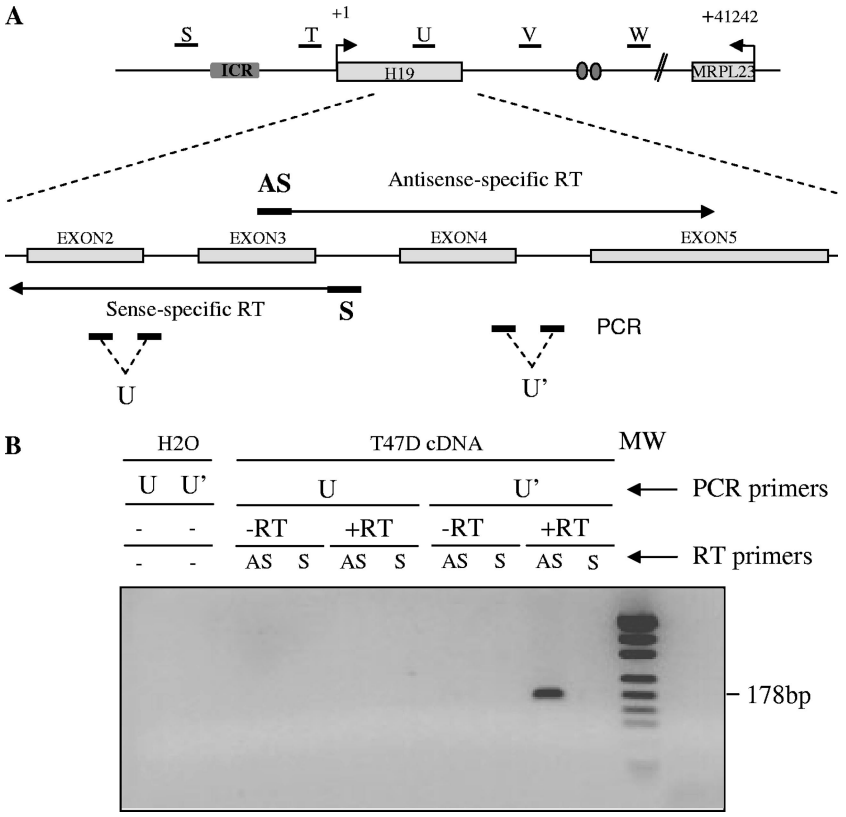

FIG. 2. Transcriptional orientation of the intergenic transcriptional activity at the *H19* locus. (A) Map of the *H19* locus. Black lines indicate the five regions (named S to W) where antisense transcription has been established using strand-specific reverse transcription and real-time PCR. Below the map of the *H19* locus, the strategy used to analyze transcriptional orientation at the U region is depicted. The same strategy was used to analyze the S, T, V, and W regions. The locations of strand-specific primers used for reverse transcription (primer AS is sense to *H19*, and primer S is antisense to *H19*) and PCR amplifications (U and U' amplifications) are indicated. Strand-specific primers were used for reverse transcription on total RNA samples from T47D cells. Real-time PCRs were then performed on each side of the RT priming region to identify the orientation of *91H* (U and U' PCR amplifications). (B) Agarose gel of PCR products obtained for the U region with the different RT-PCR combinations. Only RT analyses performed to detect antisense RNA (primer AS) gave significant PCR amplification and only when PCR amplified by the U' primer pair. To exclude any gDNA contaminations, we analyzed RT reactions performed without RT (–RT), and we ascertained the absence of self-priming analyzing reverse transcription performed without any strand-specific primers (H_2O). The results obtained for the S, T, V, and W regions can be seen in Fig. S2A in the supplemental material. The primer sequences are available in Table S1 in the supplemental material.

an *H19* antisense-specific probe in breast cancer cell lines and tumor biopsies but not in normal breast cells or normal biopsies (data not shown).

The antisense *H19* transcription defines a new transcript: the *91H* RNA. To further characterize the antisense *H19* transcription, we then mapped its 5′ and 3′ limits. In humans, the 5′ limit is located within intron 1 of the *MRPL23* gene (Fig. 3A and B), a gene located ~40 kb downstream of *H19*, which is transcribed in an opposite transcriptional orientation (Fig. 2A). Indeed, on total cDNA, we detected transcripts in the 3′ flanking region of *MRPL23* gene (MrpA amplification), as well as within the *MRPL23* region (MrpC and MrpD amplifications), but not in the promoter region of *MRPL23* gene (MrpG amplification) (Fig. 3B, total cDNA column). PCR amplifications performed on strand-specific RT with a MrpB primer (Fig. 3A and B) formally exclude any interference with *MRPL23* pre-messengers and showed that the 5′ limit of the antisense *H19* transcription is located within *MRPL23* intron 1, between MrpE and MrpF amplifications, about 3,000 to 1,900 bp downstream of the *MRPL23* transcription start site. To define the precise beginning of the *91H* transcript, we performed 5′RACE-PCR experiments. We performed PCR with specific primers, and we verified the specificity of the amplification by nested PCR. Cloning and sequencing of the PCR fragments obtained (Fig. 3C) confirmed that the transcription start site was located in intron 1 of the *MRPL23* gene at bp 47348 of the transcription start site of *H19*. To identify transcriptional regulatory sequences, we analyzed the 5′-flanking region from 500 bp upstream of the transcription start site with a predicting computer program (TFsearch and AliBaba). The sequence analysis failed to identify a TATA-box (Fig. 3D), but we identified several putative E2F binding sites that are also known to regulate *H19* expression (3). AML-1a, GATA-1/2, N-Myc, and other putative binding sites were also detected (Fig. 3D). Elsewhere, we found that the 3′ limit was located about 70 kb upstream of *H19* (Fig. 3E and F). Indeed, transcriptional activity has been detected on total cDNA with amplifications IgfA and IgfB but not with amplifications IgfC to IgfG. 3′RACE-PCR experiments mapped the 3′ end at bp -72044 relative to the *H19* transcription start site (Fig. 3G and

A

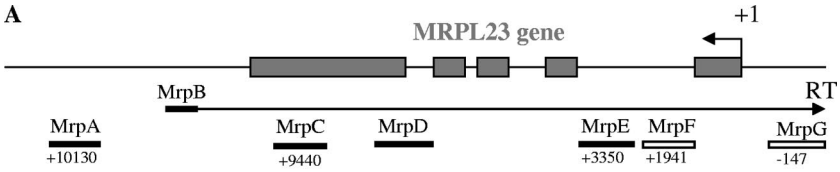

B

PCR	gDNA	Total cDNA	MRPL23 Sense-Specific cDNA
MrpA	23.45	34.94	nd
MrpC	26.37	31.78	26.98
MrpD	23.35	34.79	27.59
MrpE	26.01	nd	30.67
MrpF	22.37	nd	No Ct
MrpG	28.90	No Ct	No Ct

C

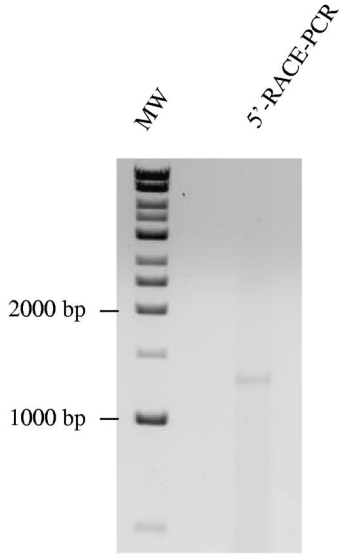

D

```
-636 gccggcagtg gcaggggcgg gaacgggggt gggggacggt aggacggtgc tgcctgtcca
                SP1                  MZF1
-576 cccagctgaa cgtgggagaa tgcacgaaac caactggcta gagattctgc acgatcgtca
                          E2F                                GATA-1/GATA-2
-516 cctggccccc cagcccaggc agcgtgctgg tctagtttgc ggtggccact tggcacctct
                                                AML-1a      Nkx-2
-456 ccatctgcct ctgctggctt ttagtggagt gctggggtgt ggtgcactca actcacattt
   GATA-1/GATA-2                              AML-1a AML-1a       AhR/Arnt
-396 agtgtactga atcagagtct tggcagcacc gtcttccagg agcctaagcc tggttagcct
               AP-1
-336 gcgttctcca taccgaggag ctaggccctg ctgccaccgg gagagtgcgg agctggcctt
                                             NRF-2
-276 ttctgtccca tggtgtgtgg ttctctgcag ctccacttca cccgagcagc aggagagtgg
      CdxA              AML-1a               Nkx-2
-216 gccggccgcg tggggtctgc tctcccaggg gtatcagtgc cccaacacac gtctttgagc
                 AML-1a
-156 cttgccatca gcttattggg ggaatgctgt ctgcggggtt ctgatttttg tccattggcc
       GATA-1/GATA-2      STATx                              CdxA
 -96 ttttctaaag tctgaccttg ggggtcaaca gcgcatgctc cttaagtcga tgctagggac
      CdxA
 -36 tggccgtcca ccttggcagg cccatgtgag aaaggggctg tgggggacctc tgtgtccttg
                                             MZF1          GR
 +25 ggtggtgacc tgctgatagc taccccgttt cccgcccacc cctgttgtga gtggacacgc
                GATA-1/GATA-2        E2F                          N-Myc
 +85 ggggggtctgc agggttagct accctgtttc ccgcccaccc ctgttgtgag tggacacgcg
                                      E2F                          N-Myc
+145 ggggtctgca gggttagcta ccctgtttcc cgcccaccac tgttgggagt ggacacgcgg
                                      E2F      AML-1a              N-Myc
+205 gggtctgcag ggttagctac cccgtttccc gcccaccact gttgggagtg gacactcagg
                                      E2F      AML-1a
```

E

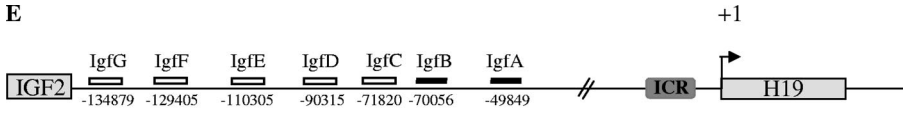

F

PCR	gDNA	Total cDNA
IgfA	22.11	31.66
IgfB	25.15	35.31
IgfC	20.34	No Ct
IgfD	26.58	No Ct
IgfE	22.35	No Ct
IgfF	22.48	No Ct
IgfG	25.79	No Ct

G

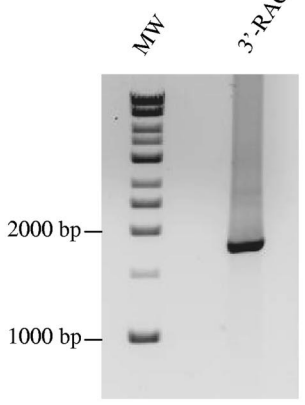

H

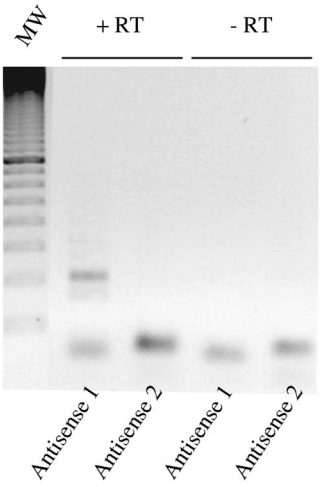

I

```
                                                    +1
    +36 acccccacc catcccaccc cctccctcac cctgctcctc ggt.....
                                H19 gene
                                          sense
 -71845 aaaatcatag ctgagcccag cctgtctgga acatgctcag agcactcaca ctagcctggc

 -71905 tgactggggg ctgtggctcg cggttgccca gcagcttcat gagacaatat tctacttcag
 -71965 gtcactagcc tgggaaaacg tcaaaattcc agatttgaag tatggcttct actgaatgca
           antisense 1                                      antisense 2
 -72025 catcactttc acaccattgt aaaaaaaaat tgtaagttga accattgtaa gtcagggact
                          end of 91H gene
 -72085 gactgtactc cgttctctaa tctccattct gcacgctcca ttttccatgt gct.....


-134865 taattgggga taatttgggg ggagggtatg tgaagggtgt tta.....
                           end of IGF2 gene
```

FIG. 3. Determination of the 5′ and 3′ limits of the antisense *H19* transcription. (A) Map of the *MRPL23* gene region. The relative positions of the PCR amplifications and strand-specific primer used for reverse transcription (MrpB) are indicated. (B) Table indicates cycle thresholds obtained in real-time PCR for each PCR amplifications on total cDNA (random priming of the RT) or after strand-specific reverse transcription with MrpB primer. gDNA is used as a positive amplification control to assess for the amplification efficiency. (C) Determination of the transcription start site of the *91H* gene by 5′RACE-PCR. RACE-PCR using T47D cell cDNA and *91H* specific primers resulted in the amplification of an ~1,300-bp DNA fragment. This fragment was cloned into TOPO plasmid for sequencing. (D) Nucleotide sequence of the 5′ region of the *91H* transcript. The transcription start site is indicated by a black arrow. Putative transcription factor binding sites identified by computer analysis are underlined. (E) Map of the *H19*/*IGF2* locus. Boxes indicate PCR amplifications used to determine the 3′ limits of the antisense transcription. Successful amplifications are depicted by full boxes, whereas abortive amplifications are shown as open boxes. (F) A table indicates the cycle thresholds (Ct) obtained for each PCR amplification. (G) Determination of the 3′ end of the *91H* RNA by 3′RACE-PCR. RACE-PCR using T47D cell cDNA resulted in the amplification of an ~1,750 bp-DNA fragment. This fragment was cloned into the TOPO plasmid for sequencing. (H) Confirmation of the 3′ end of *91H*. RT-PCRs were performed with the primer pairs depicted in panel I: sense plus antisense 1 or sense plus antisense 2. (I) Nucleotide sequence of the 3′ region of the *91H* transcript. The *H19* and *IGF2* genes are indicated in boldface, and the 3′ limit of *91H* is pointed out by a black line. Positions relative to the *H19* transcription start site (+1) are indicated. Primer sequences can be seen in Table S1 in the supplemental material.

TABLE 1. Cellular localization of human *91H*[a]

Gene	Nuclear cell extract	Cytoplasmic extract
Rplp0	20.44	**79.56**
Gapdh	21.4	**78.6**
U3 snoRNA	**73.6**	26.4
H19	44.4	55.6
91H (G primers)	**81.82**	18.18
91H (H primers)	**80.12**	19.88
MrpL23	20.83	**79.17**

[a] Relative RNA levels were determined by quantitative RT-PCR after separation of the nuclear and cytoplasmic compartments. *MrpL23*, *Rplp0*, *Gapdh*, and *H19* RNAs were used as cytoplasmic control transcripts, and *U3 snoRNA* was used as a nuclear control RNA. *91H* was quantified independently at the G and H regions (see Fig. 1). *H19* and *MrpL23* were detected using primers designed over exon/exon junctions. Values in boldface indicate the preferential localization of the transcript.

I). We confirmed these data by PCR using primers located on each side of the 3′ end, and we obtained amplification only with the sense and antisense 1 primer pair, but no fragment could be detected with the sense and antisense 2 primer pair (see Fig. 3H). Thus, antisense *H19* transcription was detected throughout a large portion of the *H19*/*IGF2* locus and has the potential to produce a single 119.392-kb transcript that we named the *91H* RNA.

***91H* RNA is a nuclear transcript.** RNA levels from nuclear and cytoplasmic extracts of T47D cells were assessed by quantitative RT-PCR to test the cellular localization of *91H*. The efficiency of the fractionation was checked by quantifying two cytoplasmic mRNAs (*RPLP0* and *GAPDH*) and a nuclear RNA (*snoRNA U3*). Using G and H primer pairs (Fig. 1), we found that *91H* RNA is almost exclusively located in the nucleus (>80%). As a control, *MRPL23* mRNA localization was analyzed and found to be mainly cytoplasmic. However, the *H19* RNA had an equal repartition in both compartments (Table 1).

***91H* overexpression in breast cancer.** *91H*, *H19*, and *IGF2* expression levels were determined by real-time RT-PCR on total RNA samples from three cancer cell lines (MCF-7, T47D, and BT20) and NBEC coming from three patients (Fig. 4A to C). *91H* and *H19* RNAs were preferentially expressed in cancer cell lines relative to noncancerous cells (Fig. 4A and B), whereas *IGF2* was strongly expressed in normal epithelial cells and displayed lower expression levels in cancerous cell lines (Fig. 4C).

We carried on our investigations by an in vivo study in normal and cancerous human breast tissues (Fig. 4D to F). *H19* and *IGF2* expression was found to be heterogeneous (Fig. 4E and F) but, more interestingly, *91H* was strongly and systematically overexpressed in all cancerous tissues examined compared to normal breast tissues (Fig. 4D). Altogether, these results indicate that *91H* RNA is consistently overexpressed in breast cancer.

***91H* stabilization in human cancer cells.** One possibility to explain *91H* RNA accumulation in cancer cells may be that it results from a stabilization of the *91H* transcripts in these cells. To determine the stability of *91H* RNA, inhibition of total cellular transcription by actinomycin D was used. *MYC* was chosen as a control for short half-life mRNA (Fig. 5B and D). Figure 5A and C shows the results from a quantitative RT-PCR analysis in normal and cancer cells treated from 30 min to 4 h with actinomycin D demonstrating that *91H* RNA half-lives were dramatically increased in T47D cancer cells (>4 h) compared to normal cells (about 30 min). The same results were obtained in BT20 cells (data not shown). Therefore, *91H* RNA accumulation in cancer cells likely results from transcript stabilization.

***91H* RNA is monoallelically expressed.** Using a polymorphic AluI restriction site available in T47D cells, we performed allelic expression analyses of both the *H19* and *91H* RNAs. Strand-specific reverse transcriptions were performed on total RNA from T47D cells and PCR amplified with primers flanking the AluI polymorphic restriction site as indicated in Fig. 6 (and Fig. S3 in supplemental material). Amplification fragment on *91H*-specific RT is resistant to AluI digestion showing that this RNA is exclusively expressed from the parental allele that does not have the AluI site (Fig. 6, left panel). Amplifications performed on *H19*-specific RT are not digested (Fig. 6, right panel) showing that *H19* RNA expression occurs on the same allele. Therefore, since *H19* RNA is known to be maternally expressed, we conclude that *91H* RNA is also produced from the maternal allele.

***91H* RNA is conserved in mice.** Using RT-PCRs on total RNAs extracted from perinatal mouse liver and heart tissue, we showed that seven intergenic regions of the *H19* locus (mA to mG, Fig. 7A) are transcribed (data not shown). In the livers of neonates, the regions located between the *H19* gene and the endodermic enhancers display expression patterns similar to those of the *H19* RNA itself (see Fig. S4A in the supplemental material). In the heart, relative to *GAPDH*, the *91H* RNA levels are similar to those observed in liver, but they appear to be almost constant from embryonic day 18.5 to 12.5 days after birth (see Fig. S4B in the supplemental material).

We also examined the transcriptional orientation of the intergenic transcription in both postnatal mouse livers and hearts. The region upstream of the endodermic enhancers (mE) was tested for transcriptional orientation (see Fig. S2B in the supplemental material). Similar to the case in humans, the transcript is antisense to *H19* in both tissues. We conclude that the *91H* RNA is conserved in the mouse.

It was then of interest to determine whether, as observed in humans, the mouse *91H* RNA was transcribed preferentially from one parental allele. We used a hybrid mouse (*Mus musculus domesticus* female × SDP711 or the reverse cross) to provide allele-specific restriction sites. SDP711 is a congenic mouse strain that has the distal part of chromosome 7 from *Mus spretus* origin). We first assessed *91H* RNA allelic expression in *H19* exon 5. In agreement with data obtained in humans, an *M. spretus*-specific BglI restriction site (Fig. 7A) allowed us to show that, in 5-day-old mouse liver, *91H* RNA is expressed almost exclusively from the maternal allele (Fig. 7B). However, using an XbaI *M. domesticus*-specific restriction site located between the two endodermic enhancers, we show that the *91H* RNA is expressed on both alleles in postnatal liver (Fig. 7C) and heart (data not shown). Elsewhere, as the regions located near the ICR (mA and mB) were recently found to be paternally transcribed (9, 42), we also determined the allelic expression in this region. While, within the ICR, some expression can be detected on the paternal allele, *91H* RNA expression is only detected on the maternal allele in the

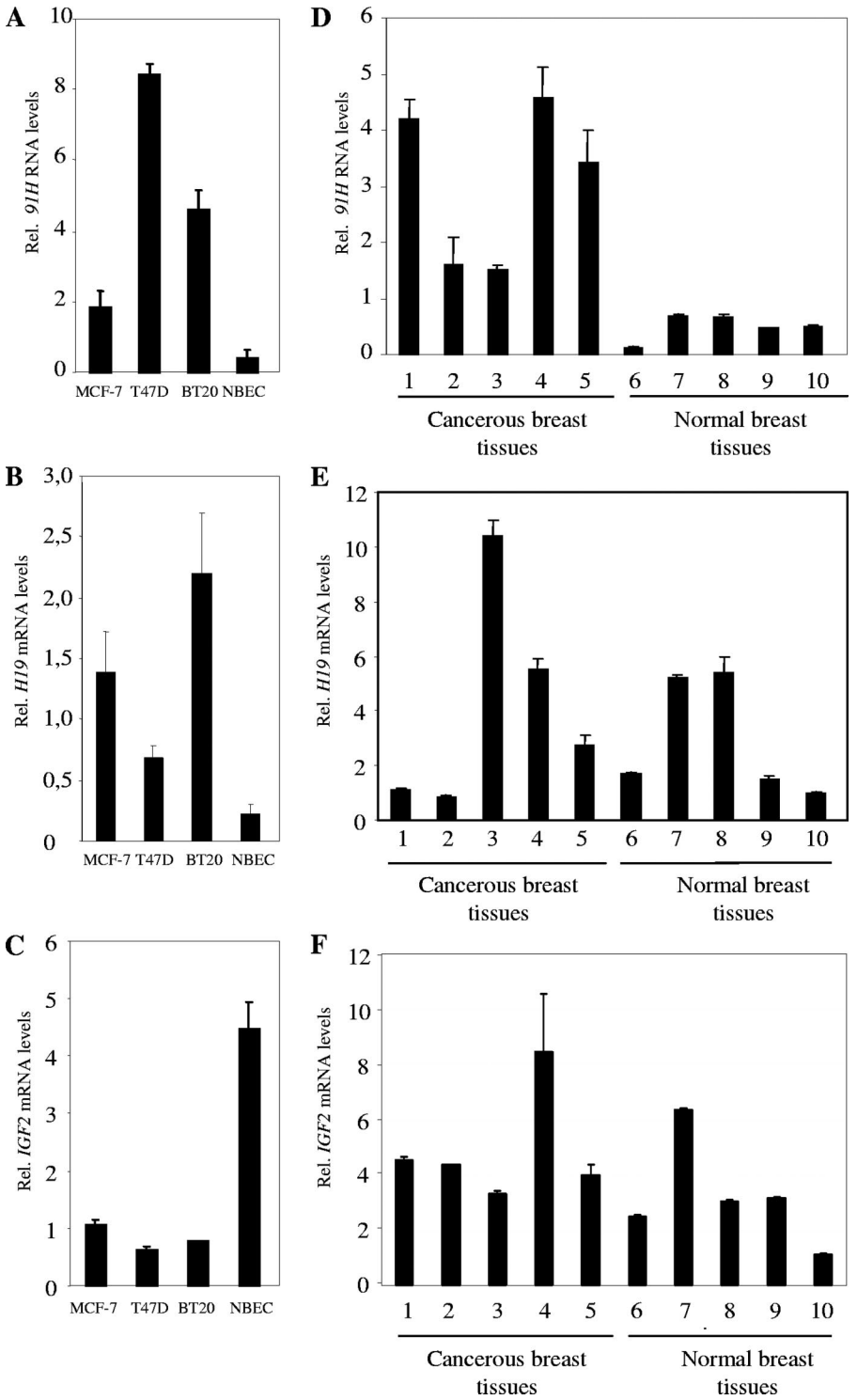

FIG. 4. *91H* expression is upregulated in breast cancer. (A to C) *91H* RNA levels (A), *H19* mRNA levels (B), and *IGF2* mRNA levels (C) in human breast cells. RNA levels were determined by real-time RT-PCR on total RNA samples from three cancer cell lines (MCF-7, T47D, and BT20) and NBEC. (D to E) *91H* RNA levels (D), *H19* mRNA levels (E), and *IGF2* mRNA levels (F) in human normal and cancer breast tissues. Expressions were normalized on *RPLP0* gene expression. *H19* RNA sense levels were quantified by using primers designed over exon/exon junctions, and *91H* was detected with the H primer pair previously described.

intergenic region located between the ICR and the *H19* gene (see Fig. S5 in the supplemental material).

In C2C12 myoblasts, *91H* RNA is upregulated upon induction of myoblastic cell differentiation (see Fig. S4C in the supplemental material). *91H* RNA levels are always much lower than those of the *H19* RNAs. They are 4 to 5 orders of magnitude less abundant than *H19* RNA levels and 10 to 100 times less abundant than *H19* precursor RNAs. In mouse myo-

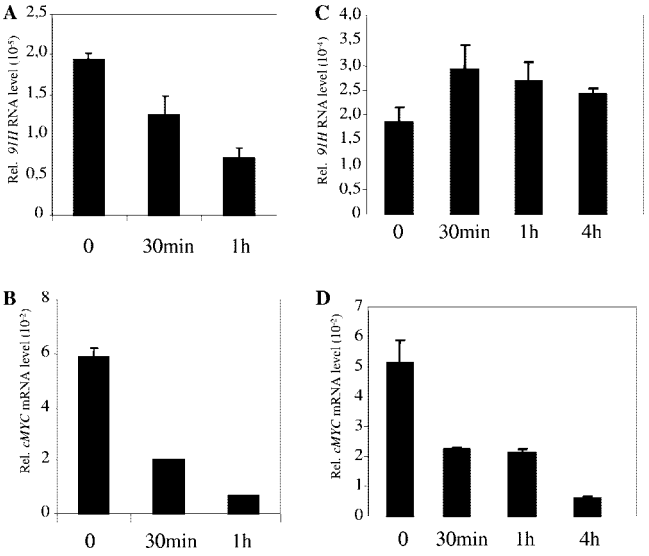

FIG. 5. *91H* RNA stability in cancer and normal breast cells. Cells were treated with 5 μg of actinomycin D/ml, and RNA levels were determined by real-time RT-PCR at the indicated times. *cMYC* was used as a positive control for actinomycin D treatment since this mRNA is known to be very unstable. *91H* (A) and *cMYC* (B) RNA levels were determined in NBEC. *91H* (C) and *cMYC* (D) RNA levels were determined in T47D cancer cells.

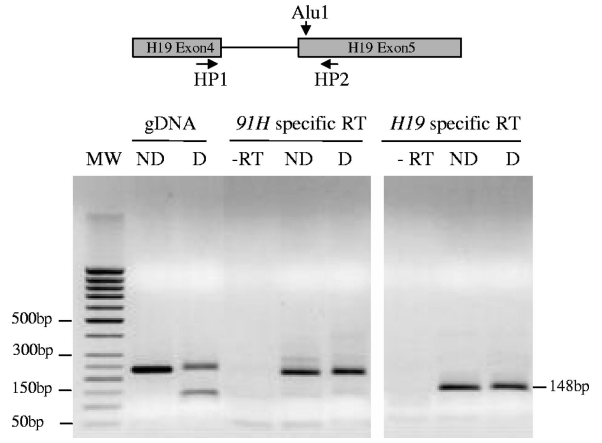

FIG. 6. Allelic expression analysis of the human *91H* RNA. Strand-specific reverse transcription was performed on total RNA from T47D cells with a reverse primer for *H19*-specific RT and a forward primer for *91H*-specific RT (see the Materials and Methods). PCR were performed with primers located on each side of the AluI polymorphic restriction site as indicated in the figure (HP1 and HP2). The PCR products were then digested with AluI and separated into agarose gel. Note that, as expected, the size of the *H19* amplification fragment is smaller than those obtained for *91H* RNA amplification because of the removal of the 81-bp *H19* intron 5 in the *H19* RNA. ND, not digested; D, AluI digestion; –RT, amplifications on control reactions made without reverse transcription. gDNA, control amplification on T47D cell gDNA.

blastic C2C12 cells, the half-life of *91H* was found to be very short since *91H* RNA is largely depleted after 15 min of actinomycin D treatment, whereas *H19* RNA shows no significant changes after 4 h of treatment (data not shown). Therefore, because of its short half-life and even if the *91H* RNA levels are rather weak, *91H* transcriptional activity may be important. Finally, in mouse proliferating and differentiated myoblastic C2C12 cells, we confirmed the nuclear localization of *91H*, whereas the *H19* RNA was mainly cytoplasmic (Table 2).

***91H* silencing decreases *IGF2* expression.** To check whether the antisense RNA had a role in the imprinting or gene expression at the *H19/IGF2* locus, *91H* RNA levels were downregulated by using two siRNAs (si*91H* 1 and 2 [Fig. 8A]). Cotransfection of the siRNA alone or in combination in T47D cells induces a strong decrease of *91H* RNA levels (Fig. 8B) and a slight decrease in *H19* RNA levels (Fig. 8C). Similar results were obtained in BT20 and PC3 cell lines (data not shown). Using a polymorphic AluI site for *H19* in T47D cells, we assessed that *H19* imprinting was not altered (see Fig. S6 in the supplemental material). Interestingly, *IGF2* mRNA levels were twofold lower after si*91H* treatment (Fig. 8D). These results suggest thus that the reduced expression of *IGF2* in siRNA-treated cells depends on interference directed against *91H* nuclear transcripts. Since no informative polymorphic restriction site was available to investigate *IGF2* allelic expression in T47D cells, we used PC3 cells in which we found a polymorphic ApaI site located in exon 9 of the *IGF2* gene. In these cells, we also observed an ~50% reduction of *IGF2* expression after si*91H* treatment (data not shown). Combining RT-PCR performed on cDNA from siRNA-treated cells and ApaI restriction, we showed that both *IGF2* parental alleles are expressed (Fig. 8E). This result may be explained by a loss of *IGF2* imprinting on the maternal allele. However, since *IGF2* mRNA levels are weak in these cells and because they are decreased in siRNA-treated cells, we suspected that it may rather reflect a reduction of *IGF2* expression on the nonimprinted paternal allele, thus uncovering a transcriptional leakage observed on the maternal allele. Using a previously described allele-specific quantitative RT-PCR technique (51), we demonstrated that downregulation of the *91H* RNA by siRNA leads to a decrease of *IGF2* expression exclusively on the paternal ApaI allele (Fig. 8F). Since this allele is the one that is preferentially expressed in PC3 cells, we can thus reasonably assume that it corresponds to the paternal allele.

DISCUSSION

Antisense transcription is a widespread phenomenon in eukaryote genome. In recent years, natural noncoding antisense transcripts have been implicated in many aspects of eukaryotic gene expression, including genomic imprinting, RNA interference, translational regulation, alternative splicing, X-inactivation, and RNA editing (20). We have identified here a new antisense transcript that we named *91H*, at the human and mouse *H19/IGF2* locus. It shares similar characteristics with well-known ncRNAs such as the *Air* transcript (43). Indeed, *91H* RNA corresponds to a short-lived and 120-kb-long transcript, overlapping the *H19* imprinted gene, the nonimprinted flanking gene *MRPL23* (55), and intergenic regions including the ICR. Its transcription start site is located at bp 47348 relative to the transcription start site of the *H19* gene, and the 3′ end is found at bp −72044 relative to the transcription start site of the *H19* gene. It is localized to the nucleus, and its promoter lies in an intron of an active host mRNA gene, such as the *Air* promoter that is located in the second intron of the

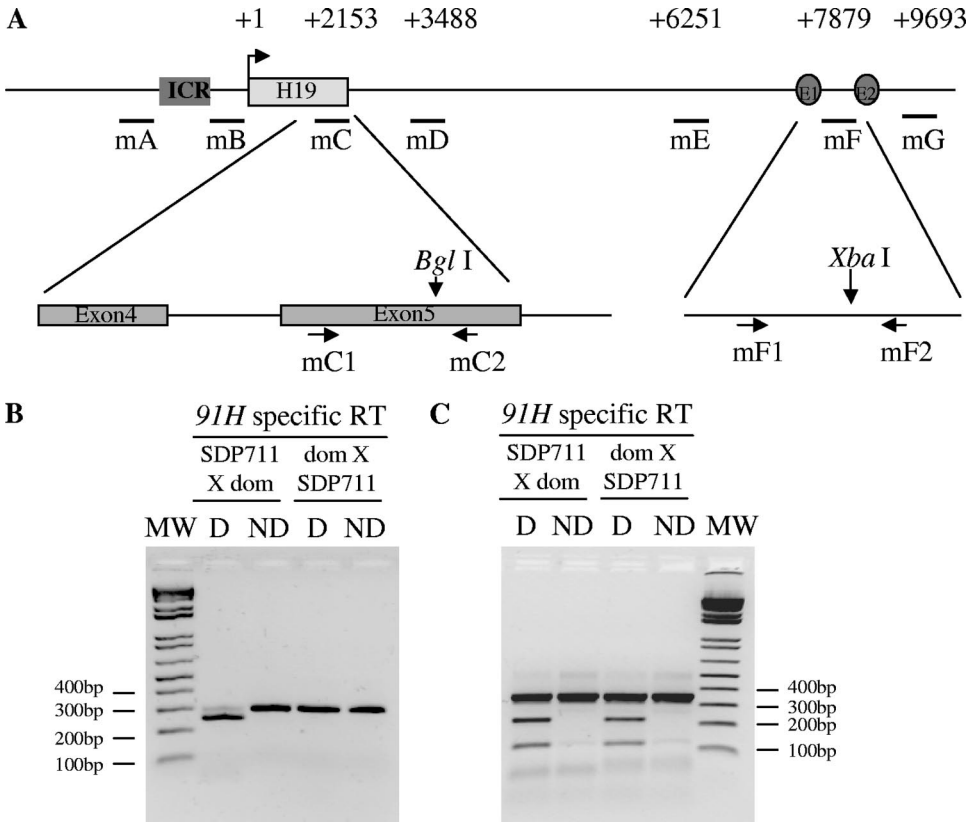

FIG. 7. Allelic expression of the murine *91H* RNA. (A) Map of *H19* region indicating positions of PCR primer pairs used in real-time PCR (mC1 and mC2; mF1 and mF2). (B) RT using a *H19*-sense-intron 4 primer was performed on total RNA extracted from 5-day-old mouse liver issued from *SDP711XM.m.dom*. (left panel) or *M.m.dom.XSDP711* hybrid mice (right panel). A 301-bp PCR fragment was then obtained by using the mC primer pair and digested (D) or undigested (ND) with BglI at an *M. spretus*-specific restriction site. (C) Reverse transcription using an mF1 sense primer was performed on the samples described above. A 344-bp PCR fragment was then obtained using the mF primer pair and cut by XbaI at a *M. musculus domesticus*-specific restriction site.

Igf2r promoter, showing that transcription of the ncRNA promoter does not interfere with expression of the host mRNA gene.

Interestingly, *91H* RNA shows an increased stability in cancer cells, leading to its accumulation in cancer cell lines and breast cancer tissues. This transcript stabilization is reminiscent of the previously described stabilization of the *H19* ncRNA, which is responsible for its accumulation during in vitro muscle cell differentiation (29).

TABLE 2. Cellular localization of mouse *H19* in proliferative and differentiated C2C12 myoblastic cells[a]

Gene	C2C12 cells (relative % total expression)			
	Proliferating		Differentiated	
	Nuclear cell extract	Cytoplasmic cell extract	Nuclear cell extract	Cytoplasmic cell extract
U3 snoRNA	**68**	32	**94.2**	5.8
H19	23.6	**76.4**	16.6	**83.4**
91H (mE primers)	**100**	<0.05	**99.5**	<0.5
91H (mG primers)	**100**	<0.05	**100**	<0.05

[a] RNA levels were determined as described for Table 1. The results are expressed in relative percentages of total expression. Values in boldface indicate the preferential localization of the transcript.

We noticed a preferential *91H* expression on the maternal allele in both mice and humans within the *H19* gene region (Fig. 6 and 7) and between the ICR and the *H19* cap site (Fig. S5B in the supplemental material). However, we detected a biallelic transcription in the 3′ endodermic enhancers region (Fig. 7C) and in the ICR in mouse (Fig. S5A in the supplemental material) according to the results obtained by Drewell et al. (9) and Schoenfelder et al. (42), who demonstrated biallelic sense and antisense transcription in the mouse *H19* ICR. These data show that, in the mouse, some regions, and particularly regulatory regions, probably generate transcription independently of *91H*. However, in humans, using a HhaI polymorphic site, we only detected monoallelic antisense transcription in the ICR (Fig. S7 in the supplemental material).

The developmental expression patterns of *91H* are very similar to those of the *H19* RNA in murine liver, and both RNAs are upregulated upon induction of myoblastic cell differentiation. This suggests that both transcripts are subject to a common regulation of the locus which allows gene transcription in a time-restricted manner.

To address the functional role of the antisense transcript, we knocked down its expression by RNA interference assays in human cells. The results indicated that, whereas *91H* silencing does not modify *H19* imprinted status and slightly affects *H19*

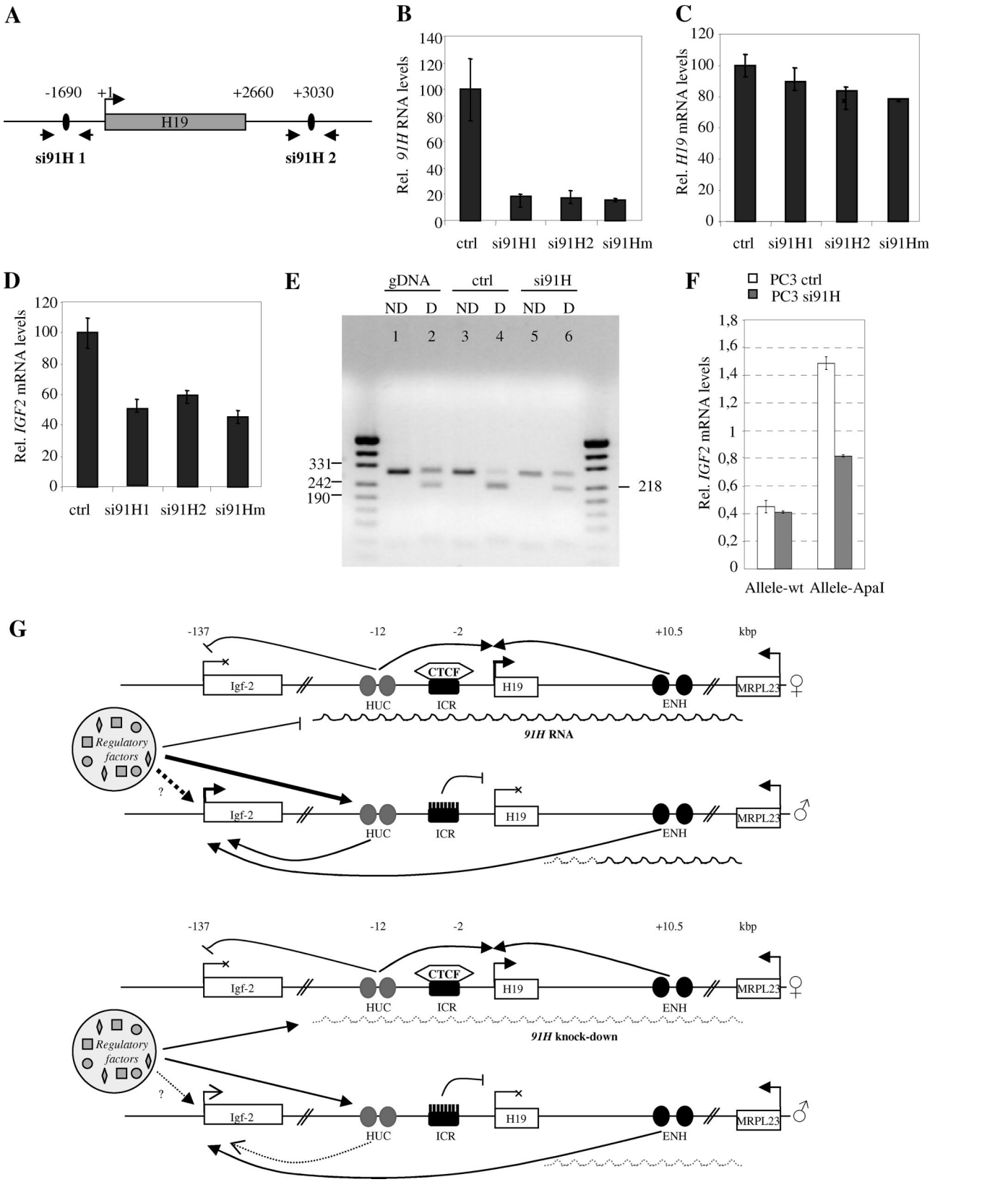

FIG. 8. *91H* silencing by RNA interference reduces *IGF2* expression on the paternal allele. (A) Map of *H19* region indicating the positions of siRNA sequences and the PCR primer pairs used in real-time PCR. T47D cells were transfected with siRNA targeting either the green fluorescent protein (ctrl) or the *91H* RNA (si*91H* 1 and 2 alone or in combination). *91H* (B), *H19* (C), and *IGF2* (D) RNA levels were determined by real-time RT-PCR 24 h after transfection. The results were normalized to *RPLP0* expression levels. (E) PC3 cells were transfected with si*91H*, and the

expression, it strongly reduces the overall *IGF2* mRNA levels. It was therefore somewhat surprising that semiquantitative RT-PCR detected transcriptional activity on both *IGF2* alleles in siRNA-treated cells. To reconcile these data, we assumed that this *IGF2* reexpression from the maternal allele may rather reflect a transcriptional leakage that was underestimated in untreated cells because of a high expression level on the paternal allele. Indeed, allele-specific quantitative RT-PCR demonstrated that downregulation of the *91H* RNA leads to a decrease of *IGF2* expression exclusively on the paternal allele. Therefore, we conclude that, in humans, *91H* RNA produced from the maternal chromosome does not affect genomic imprinting but is involved in the maintenance of *IGF2* gene expression in *trans* on the paternal allele. Importantly, two distinct siRNA probes, targeting different regions of the *91H* transcript and used in separate experiments have identical effects on *Igf2* mRNA levels. Therefore, the possibility that the siRNA probes interfere with known *cis*-acting regulatory DNA elements is very unlikely. *IGF2* upregulation through a *trans* effect by ectopic expression of *H19* antisense transcripts has been suggested (53). The fact that *91H* knockdown only slightly affects *H19* gene expression from the maternal allele seems to indicate that the *91H* effect is not mediated through the ICR/CTCF complex. However, other candidates such as enhancer DNA regions may be considered for interacting with the antisense RNA. Indeed, *91H* encompasses a region including a previously described nuclease hypersensitive site (approximately 30 kb upstream of the *H19* gene) that can be found on both parental alleles (2) and that have enhancer functions in both imprinted and nonimprinted tissues (6). In addition, the biallelically transcribed *H19* upstream conserved (HUC) sequences are regulatory elements located just upstream of the ICR that act as strong mesodermal enhancers and are supposed to activate *IGF2* expression on the paternal allele (9).

The *91H trans* effect may reflect a competition model that explains a communication between both parental chromosomes that we evoked in a previous work (11). Indeed, deletions of the active maternal allele of the *H19* gene reduce the paternal *IGF2* DMR2 methylation level and therefore probably have both *cis* and *trans* effects on *IGF2* gene expression. These results are consistent with the present study and may be due to *91H* transcript disruption. Elsewhere, it has been demonstrated that ncRNAs are able to guide the epigenetic regulation of genes. For the human *HOX* loci, their expression demarcates broad chromosomal domains of differential histone methylation and RNA polymerase accessibility (37). In particular, the *HOTAIR* ncRNA located in a regulatory boundary in the *HOXC* cluster represses transcription in *trans* across 40 kb of the *HOXD* locus. This ncRNA binds to an epigenetic regulatory complex and changes the methylation patterns of the target locus. We then proposed a model to explain the *91H trans* effect on *IGF2* expression in which cooperation between two sets of enhancer sequences would be required for full expression of the gene. In addition, both parental alleles would be competing for a common limiting pool of regulatory factors. In this model, *91H* would be essentially involved in modifying the accessibility of HUC sequences to regulating proteins. Indeed, maternal expression of *91H* would preferentially direct regulatory elements on the paternal allele within the HUC region. This region would cooperate with ENH sequences, resulting in paternal *IGF2* enhanced expression (Fig. 8G). We cannot exclude the intervention of other enhancer sequences that may be responsible for the *trans* effect of *91H* RNA on *IGF2* expression (18).

Elsewhere, *91H* may attract repressive chromatin modifications to the maternal allele by trapping factors responsible for DNA or histone modifications that become available for the paternal allele when *91H* is disrupted, resulting in *IGF2* expression decrease. Yu et al. (52) recently showed that many tumor suppressor genes have nearby antisense RNAs. These authors focused on the *p15* antisense RNA, which is able to induce *p15* gene silencing through heterochromatin formation (increase in dimethylation of H3K9 and decrease in dimethylation of H3K4). Thus, it will be useful to analyze histone methylation and/or acetylation patterns of the paternal *IGF2* region in the presence or in the absence of the *91H* RNA.

Other authors have already evoked this type of *trans* regulation within an imprinted locus. Takeda et al. (46) examined the callipyge phenotype (postnatal muscular hypertrophy of shape) caused by a mutation in the *DLK1-GTL2* locus. The mutation and its "polar overdominance" mode of inheritance imply that only the heterozygous animals that have received the paternal mutation display the phenotype. The mutation, when paternally inherited, increases DLK1 and PEG11 protein levels, which results in the callipyge phenotype. However, in the case of a double maternal and paternal inherited mutation, it was suggested that the overexpression of ncRNAs from the maternal allele could inhibit in *trans* the translation of *DLK1* and *PEG11* genes, resulting in a normal phenotype. This *trans* inhibition have been formally demonstrated for *PEG11* through a maternal miRNA. For *DLK1*, these authors propose that the posttranscriptional inhibition may be mediated by a

imprinting status of the *IGF2* alleles was examined using a RT-PCR amplification digested (D) or undigested (ND) with an ApaI polymorphic restriction site available in this cell line. (F) The *IGF2* expression levels were determined on each parental allele using an allele-specific RT-PCR amplification method (51) from PC3 cells transfected with control siRNA or with si*91H*. (G) Model for *91H trans* effect on *IGF2* expression. Two sets of enhancers (HUC and ENH sequences) regulate *IGF2* expression. Both would be required for full expression of the gene. In addition, the two *IGF2* alleles would be competing for a common limited stock of regulatory elements (methylation/acetylation/transcription?). On the maternal allele, *91H* would block the locus and prevent the HUC sequences from interaction with any regulatory factors. These would be then directed on the paternal allele, in the HUC region, and/or in the *IGF2* promoter region and would cooperate with the *cis* endodermic enhancers, resulting in *IGF2* enhanced expression. Upon siRNA treatment and *91H* knockdown, the competition would be lost and, as a consequence, both *IGF2* alleles would be now able to interact with the regulatory factors with similar efficiencies. Because these factors are in a limiting amount, a part would be depleted from the paternal *IGF2* allele to interact with the maternal allele. This would lead to a paternal *IGF2* expression decrease but unchanged maternal *IGF2* expression because of the absence of functional ENH sequences. Arrows indicates positive regulations, whereas lines with bars correspond to inhibitions.

long ncRNA which could, for instance, compete toward a *trans* factor responsible for *DLK1* RNA localization or translation. Our model shares interesting similarities, although the *trans* regulation affecting DLK1 protein levels is different from those affecting *IGF2* transcripts accumulation after *91H* knockdown.

Interestingly, and in agreement with the role of *91H* displayed in PC3 cells, we noticed an inverse correlation between *91H* and *IGF2* transcription in normal and cancer mammary cell lines. However, in breast cancer tissues, whereas *91H* is always overexpressed, *IGF2* and *H19* expression profiles are more heterogeneous; this is probably due to various co- or posttranscriptional regulations. These data provide a link between antisense transcription and cancer.

Finally, *91H* RNA discovery leads us to reconsider some previous results. Indeed, a set of studies in the mouse described deletions of sequences within the *H19/IGF2* locus that did not affect *H19* and *IGF2* expression: deletion of the *H19* promoter and structural gene (41), deletion of a G-rich repetitive element located immediately 3′ to the ICR (48), deletion of a conserved direct tandem repeat 1 kb upstream of the ICR (23), and deletion of a 4.2-kb domain between the *H19* transcription unit and the enhancers (49). We presume that these deletions did not impede *91H* transcription and generated a transcript that could still assume its regulatory function.

In conclusion, the antisense transcript reported here adds further complexity to the cluster of imprinted genes in the human imprinted 11p15.5 region. *91H* RNA is involved in the control of *IGF2* expression in *trans*, suggesting that, beyond imprinting, other sophisticated mechanisms involved in the control of gene expression arise at this locus. Cooperation between individual regulatory elements (i.e., enhancers, silencers, antisense RNA, DNA, and histone modifications) seems to be required for fine-tuning *H19* and *IGF2* gene expression.

ACKNOWLEDGMENTS

We thank A. Béthouart, N. Nguyen, and C. Cathelineau for their collaboration in the collect of breast cancer tissues. We thank P. Pellerin (Lille Hospital, Lille, France) for its collaboration to collect breast normal tissues. We thank P. Delannoy (USTL, Lille, France) for the use of MX4000 apparatus and L. Brunet and G. Courtand (CCMIC and USTL) for their help with the text illustrations.

J.-J.C., E.A., and T.D. hold grants from the Fédération des Groupements des Entreprises Françaises dans la Lutte contre le Cancer, the Comités du Nord et de l'Aisne de la Ligue Nationale contre le Cancer, and the Association pour la Recherche sur le Cancer (ARC). N.B. is the recipient of fellowships from the Ministère de l'Education Nationale et de la Recherche, the ARC, and the Institut National du Cancer. This study was also supported by grants from the ARC (grant 4868), the GIS Longévité (contract GISLO401), the Fond National de la Science (ACI Jeune Chercheur), and the Agence Nationale de La Recherche (ANR-07-BLAN-0052-02 -T.F.-) and by funds from the Centre National de la Recherche Scientifique.

We dedicate this report to the memory of our friend Jean Coll.

REFERENCES

1. **Adriaenssens, E., L. Dumont, S. Lottin, D. Bolle, A. Leprêtre, A. Delobelle, F. Bouali, T. Dugimont, J. Coll, and J. J. Curgy.** 1998. H19 overexpression in breast adenocarcinoma stromal cells is associated with tumor values and steroid receptor status but independent of p53 and Ki-67 expression. Am. J. Pathol. **153:**1597–1607.
2. **Ainscough, J. F., T. Koide, M. Tada, S. Barton, and M. A. Surani.** 1997. Imprinting of *IGF2* and *H19* from a 130-kb YAC transgene. Development **124:**3621–3632.
3. **Berteaux, N., S. Lottin, D. Monté, S. Pinte, B. Quatannens, J. Coll, H. Hondermarck, J. J. Curgy, T. Dugimont, and E. Adriaenssens.** 2005. H19 mRNA-like noncoding RNA promotes breast cancer cell proliferation through positive control by E2F1. J. Biol. Chem. **280:**29625–29636.
4. **Bestor, T. H.** 2000. The DNA methyltransferases of mammals. Hum. Mol. Genet. **9:**2395–2402.
5. **Brannan, C. I., E. C. Dees, R. S. Ingram, and S. M. Tilghman.** 1990. The product of the *H19* gene may function as an RNA. Mol. Cell. Biol. **10:**28–36.
6. **Charalambous, M., T. R. Menheniott, W. R. Bennett, S. M. Kelly, G. Dell, L. Dandolo, and A. Ward.** 2004. An enhancer element at the *IGF2/H19* locus drives gene expression in both imprinted and non-imprinted tissues. Dev. Biol. **271:**488–497.
7. **Constancia, M., W. Dean, S. Lopes, T. Moore, G. Kelsey, and W. Reik.** 2001. Deletion of a silencer element in *IGF2* results in loss of imprinting independent of *H19*. Nat. Genet. **26:**203–206.
8. **DeChiara, T. M., E. J. Robertson, and A. Efstratiadis.** 1991. Parental imprinting of the mouse insulin-like growth factor II gene. Cell **64:**849–859.
9. **Drewell, R. A., K. L. Arney, T. Arima, S. C. Barton, J. D. Brenton, and M. A. Surani.** 2002. Novel conserved elements upstream of the *H19* gene are transcribed and act as mesodermal enhancers. Development **129:**1205–1213.
10. **Elbashir, S. M., J. Harborth, W. Lendeckel, A. Yalcin, K. Weber, and T. Tuschl.** 2001. Duplexes of 21-nucleotide RNAs mediate RNA interference in cultured mammalian cells. Nature **411:**494–498.
11. **Forne, T., J. Oswald, W. Dean, J. R. Saam, B. Bailleul, L. Dandolo, S. M. Tilghman, J. Walter, and W. Reik.** 1997. Loss of the maternal *H19* gene induces changes in *IGF2* methylation in both cis and trans. Proc. Natl. Acad. Sci. USA **94:**10243–10248.
12. **Fuks, F.** 2003. DNA methyltransferases: from chromatin remodeling to cancer. Med. Sci. **19:**477–480.
13. **Grabe, N.** 2002. AliBaba2: context specific identification of transcription factor binding sites. In Silico Biol. **2:**1–15.
14. **Grandjean, V., L. O'Neill, T. Sado, B. Turner, and A. Ferguson-Smith.** 2001. Relationship between DNA methylation, histone H4 acetylation and gene expression in the mouse imprinted *IGF2-H19* domain. FEBS Lett. **488:**165–169.
15. **Heard, E.** 2004. Recent advances in X-chromosome inactivation. Curr. Opin. Cell Biol. **16:**247–255.
16. **Heinemeyer, T., E. Wingender, I. Reuter, H. Hermjakob, A. E. Kel, O. V. Kel, E. V. Ignatieva, E. A. Ananko, O. A. Podkolodnaya, F. A. Kolpakov, N. L. Podkolodny, and N. A. Kolchanov.** 1998. Database on transcriptional regulation: TRANSFAC, TRRD, and COMPEL. Nucleic Acids Res. **26:**362–367.
17. **Ishihara, K., N. Hatano, H. Furuumi, R. Kato, T. Iwaki, K. Miura, Y. Jinno, and H. Sasaki.** 2000. Comparative genomic sequencing identifies novel tissue-specific enhancers and sequence elements for methylation-sensitive factors implicated in *IGF2/H19* imprinting. Genome Res. **10:**664–671.
18. **Kaffer, C. R., A. Grinberg, and K. Pfeifer.** 2001. Regulatory mechanisms at the Igf2/H19 locus. Mol. Cell. Biol. **21:**8189–8196.
19. **Kurukuti, S., V. K. Tiwari, G. Tavoosidana, E. Pugacheva, A. Murrell, Z. Zhao, V. Lobanenkov, W. Reik, and R. Ohlsson.** 2006. CTCF binding at the *H19* imprinting control region mediates maternally inherited higher-order chromatin conformation to restrict enhancer access to *IGF2*. Proc. Natl. Acad. Sci. USA **103:**10684–10689.
20. **Lavorgna, G., D. Dahary, B. Lehner, R. Sorek, C. M. Sanderson, and G. Casari.** 2004. In search of antisense. Trends Biochem. Sci. **29:**88–94.
21. **Leighton, P. A., J. R. Saam, R. S. Ingram, C. L. Stewart, and S. M. Tilghman.** 1995. An enhancer deletion affects both *H19* and *IGF2* expression. Genes Dev. **9:**2079–2089.
22. **Leighton, P. A., R. S. Ingram, J. Eggenschwiler, A. Efstratiadis, and S. M. Tilghman.** 1995. Disruption of imprinting caused by deletion of the *H19* gene region in mice. Nature **375:**34–39.
23. **Lewis, A., K. Mitsuya, M. Constancia, and W. Reik.** 2004. Tandem repeat hypothesis in imprinting: deletion of a conserved direct repeat element upstream of H19 has no effect on imprinting in the Igf2-H19 region. Mol. Cell. Biol. **24:**5650–5656.
24. **Lewis, A., and A. Murrel.** 2004. Genomic imprinting: CTCF protects the boundaries. Curr. Biol. **14:**284–286.
25. **Li, Y. M., G. Franklin, H. M. Cui, K. Svensson, X. B. He, G. Adam, R. Ohlsson, and S. Pfeifer.** 1998. The *H19* transcript is associated with polysomes and may regulate *IGF2* expression in trans. J. Biol. Chem. **273:**28247–28252.
26. **Lottin, S., A. S. Vercoutter-Edouart, E. Adriaenssens, X. Czeszak, J. Lemoine, M. Roudbaraki, J. Coll, H. Hondermarck, T. Dugimont, and J. J. Curgy.** 2002. Thioredoxin posttranscriptional regulation by *H19* provides a new function to mRNA-like non-coding RNA. Oncogene **21:**1625–1631.
27. **Lottin, S., E. Adriaenssens, T. Dupressoir, N. Berteaux, C. Montpellier, J. Coll, T. Dugimont, and J. J. Curgy.** 2002. Overexpression of an ectopic *H19* gene enhances the tumorigenic properties of breast cancer cells. Carcinogenesis **23:**1885–1895.
28. **Lottin, S., E. Adriaenssens, N. Berteaux, A. Leprêtre, M. O. Vilain, E. Denhez, J. Coll, T. Dugimont, and J. J. Curgy.** 2005. The human H19 gene is frequently overexpressed in myometrium and stroma during pathological endometrial proliferative events. Eur. J. Cancer **41:**168–177.
29. **Milligan, L., E. Antoine, C. Bisbal, M. Weber, C. Brunel, T. Forne, and G. Cathala.** 2000. *H19* gene expression is up-regulated exclusively by stabilization of the RNA during muscle cell differentiation. Oncogene **19:**5810–5816.
30. **Murrell, A., S. Heeson, and W. Reik.** 2004. Interaction between differentially

methylated regions partitions the imprinted genes *IGF2* and *H19* into parent-specific chromatin loops. Nat. Genet. **36:**889–893.
31. **Pandey, R. R., M. Ceribelli, P. B. Singh, J. Ericsson, R. Mantovani, and C. Kanduri.** 2004. NF-Y regulates the antisense promoter, bidirectional silencing, and differential epigenetic marks of the Kcnq1 imprinting control region. J. Biol. Chem. **279:**52685–52693.
32. **Pauler, F. M., and D. P. Barlow.** 2006. Imprinting mechanisms-it only takes two. Genes Dev. **20:**1203–1206.
33. **Peters, J., and C. Beechey.** 2004. Identification and characterisation of imprinted genes in the mouse. Brief Funct. Genomic Proteomic **2:**320–333.
34. **Pfaffl, M. W.** 2001. A new mathematical model for relative quantification in real-time RT-PCR. Nucleic Acids Res. **29:**e45.
35. **Reik, W., K. W. Brown, H. Schneid, Y. Le Bouc, W. Bickmore, and E. R. Maher.** 1995. Imprinting mutations in the Beckwith-Wiedemann syndrome suggested by altered imprinting pattern in the *IGF2-H19* domain. Hum. Mol. Genet. **4:**2379–2385.
36. **Reik, W.** 2007. Stability and flexibility of epigenetic gene regulation in mammalian development. Nature **447:**425–432.
37. **Rinn, J. L., M. Kertesz, J. K. Wang, S. L. Squazzo, X. Xu, S. A. Brugmann, L. H. Goodnough, J. A. Helms, P. J. Farnham, E. Segal, and H. Y. Chang.** 2007. Functional demarcation of active and silent chromatin domains in human HOX loci by noncoding RNAs. Cell **129:**1311–1323.
38. **Ripoche, M. A., C. Kress, F. Poirier, and L. Dandolo.** 1997. Deletion of the *H19* transcription unit reveals the existence of a putative imprinting control element. Genes Dev. **11:**1596–1604.
39. **Rougeulle, C., and E. Heard.** 2002. Antisense RNA in imprinting: spreading silence through Air. Trends Genet. **18:**434–437.
40. **Rougeulle, C., C. Cardoso, M. Fontes, L. Colleaux, and M. Lalande.** 1998. An imprinted antisense RNA overlaps UBE3A and a second maternally expressed transcript. Nat. Genet. **19:**15–16.
41. **Schmidt, J. V., J. M. Levorse, and S. M. Tilghman.** 1999. Enhancer competition between H19 and Igf2 does not mediate their imprinting. Proc. Natl. Acad. Sci. USA **96:**9733–9738.
42. **Schoenfelder, S., G. Smits, P. Fraser, W. Reik, and R. Paro.** 2007. Non coding transcripts in the *H19* imprinting control region mediate gene silencing in transgenic *Drosophila*. EMBO Rep. **8:**1068–1073.
43. **Seidl, C., S. H. Stricker, and D. P. Barlow.** 2006. The imprinted Air ncRNA is an atypical RNAPII transcript that evades splicing and escapes nuclear export. EMBO J. **25:**3565–3575.
44. **Sleutels, F., R. Zwart, and D. P. Barlow.** 2002. The non-coding Air RNA is required for silencing autosomal imprinted genes. Nature **415:**810–813.
45. **Steenman, M. J., S. Rainier, C. J. Dobry, P. Grundy, I. L. Horon, and A. P. Feinberg.** 1994. Loss of imprinting of *IGF2* is linked to reduced expression and abnormal methylation of *H19* in Wilms' tumour. Nat. Genet. **7:**433–439.
46. **Takeda, H., F. Caiment, M. Smit, S. Hiard, X. Tordoir, N. Cockett, M. Georges, and C. Charlier.** 2006. The callipyge mutation enhances bidirectional long-range DLK1-GTL2 intergenic transcription in *cis*. Proc. Natl. Acad. Sci. USA **10:**8119–8124.
47. **Thakur, N., V. K. Tiwari, H. Thomassin, R. R. Pandey, M. Kanduri, A. Gondor, T. Grange, R. Ohlsson, and C. Kanduri.** 2004. An antisense RNA regulates the bidirectional silencing property of the Kcnq1 imprinting control region. Mol. Cell. Biol. **24:**7855–7862.
48. **Thorvaldsen, J. L., M. R. Mann, O. Nwoko, K. L. Duran, and M. S. Bartolomei.** 2002. Analysis of sequence upstream of the endogenous H19 gene reveals elements both essential and dispensable for imprinting. Mol. Cell. Biol. **22:**2450–2462.
49. **Verona, R. I., and M. S. Bartolomei.** 2004. Role of H19 3′ sequences in controlling H19 and Igf2 imprinting and expression. Genomics **84:**59–68.
50. **Weber, M., H. Hagege, A. Murrell, C. Brunel, W. Reik, G. Cathala, and T. Forne.** 2003. Genomic imprinting controls matrix attachment regions in the *IGF2* gene. Mol. Cell. Biol. **23:**8953–8959.
51. **Weber, M., H. Hagege, G. Lutfalla, L. Dandolo, C. Brunel, G. Cathala, and T. Forne.** 2003. A real-time polymerase chain reaction assay for quantification of allele ratios and correction of amplification bias. Anal. Biochem. **320:**252–258.
52. **Yu, W., D. Gius, P. Onyango, K. Muldoon-Jacobs, J. Karp, A. P. Feinberg, and H. Cui.** 2008. Epigenetic silencing of tumour suppressor gene p15 by its antisense RNA. Nature **451:**202–206.
53. **Wilkin, F., J. Paquette, E. Ledru, C. Hamelin, M. Pollak, and C. L. Deal.** 2000. *H19* sense and antisense transgenes modify insulin-like growth factor-II mRNA levels. Eur. J. Biochem. **267:**4020–4027.
54. **Wutz, A., O. W. Smrzka, N. Schweifer, K. Schellander, E. F. Wagner, and D. P. Barlow.** 1997. Imprinted expression of the *IGF2*r gene depends on an intronic CpG island. Nature **389:**745–749.
55. **Zubair, M., K. Hilton, J. R. Saam, M. A. Surani, S. M. Tilghman, and H. Sasaki.** 1997. Structure and expression of the mouse L23mrp gene downstream of the imprinted H19 gene: biallelic expression and lack of interaction with the H19 enhancers. Genomics **45:**290–296.